Coherent potential approximation for charge ordering in the extended Hubbard model

A T Hoang[1,2] **and P Thalmeier**[3]

[1] Max-Planck-Institut für Physik Komplexer Systeme, Nöthnitzer Strasse 38,
01187 Dresden, Germany
[2] Institute of Physics, PO Box 429, Bo Ho, Hanoi 10000, Vietnam
[3] Max-Planck-Institut für Chemische Physik Fester Stoffe, Nöthnitzer Strasse 40,
01187 Dresden, Germany

Abstract
We study charge ordering (CO) in the extended Hubbard model with both
on-site and nearest-neighbour Coulomb repulsion (U and V, respectively)
within the coherent potential approximation. The phase boundary between
the homogeneous and charge-ordered phases for the square lattice is obtained
for different values of U. It is shown that at quarter-filling for all values of
U the CO exists only if the inter-site Coulomb repulsion V exceeds certain a
critical value which is of the order of the kinetic energy t. At finite temperature
a re-entrant transition is found in some region of V.

1. Introduction

The problem of charge ordering (CO) was already attracting the attention of physicists
at the end of the 1930s. In the low-density limit, as was first proposed by Wigner [1],
the electrons crystallize in form of a lattice in order to keep the Coulomb repulsion as
small as possible. Such a Wigner lattice is experimentally realized in a GaAs/AlGaAs
heterostructure [2]. The CO may also occur at higher electron concentration if the interaction
of electrons with spin degrees of freedom or with phonons drastically reduces the kinetic
energy [3]. Recently CO has been extensively observed in real materials at high densities:
hole ordering in rare-earth pnictides such as Yb_4As_3 [4] and CO in the unconventional spin–
Peierls material α'-NaV_2O_5 [5] and in colossal-magnetoresistance compounds, for example
$R_{2-2x}A_{1+2x}Mn_2O_7$ (R = La, Pr; A = Ca, Sr; $x \geqslant 0.5$) [6].

One of the simplest models of interacting electrons that allows for CO is the extended
Hubbard model (EHM). This model has been intensively studied both in low dimensions and
in the limit of infinite dimension, usually at half-or at quarter-filling. A variety of techniques,
such as Hartree–Fock approximation [7], perturbation theory [8], the dynamical mean-field
theory (DMFT) [9] and the slave boson approach [10], as well as numerical methods such as
quantum Monte Carlo simulation [11] and the Lanczos technique [12], have been employed.

Obviously, each of these approaches is able to describe properly only one of the relevant limits of the model and, despite the many publications devoted to the CO in solids, the physical picture of the phenomenon is far from being clear.

Recently, a melting of the charge-ordered state on decreasing the temperature has been found in $Pr_{0.65}(Ca_{0.7}Sr_{0.3})_{0.35}MnO_3$ [13] and in $La_{2-2x}Sr_{1+2x}Mn_2O_7$ ($0.47 \leqslant x \leqslant 0.62$) [14, 15]. A re-entrant transition at quarter-filling has been obtained theoretically using the EHM both with electron–phonon interaction [16] and without electron–phonon interaction [9, 12]. The present paper is devoted to a study of the boundary between the charge-ordered and disordered phases for different regimes of the temperature T, the Coulomb interactions U, V and the band filling n. A simple but physically meaningful approximation allowing us to solve this problem is the coherent potential approximation (CPA). This self-consistent approximation is recognized as the best single-site approximation for the spectral properties of disordered systems. Originally, the alloy-analogue approximation was formulated as an approximation scheme for the Hubbard model [17]. To solve the alloy problem the CPA is used as a second step. The CPA was also applied to intermediate-valence and heavy-fermion systems [18]. In the present work this approximation is used for the first time to treat the CO in the EHM.

2. Model and formalism

We consider the following Hamiltonian for the EHM:

$$H = t \sum_{\langle ij \rangle \sigma}(c_{i\sigma}^+ c_{j\sigma} + c_{j\sigma}^+ c_{i\sigma}) + U \sum_i n_{i\uparrow} n_{i\downarrow} + V \sum_{\langle ij \rangle} n_i n_j, \tag{1}$$

where $c_{i\sigma}$ ($c_{i\sigma}^+$) annihilates (creates) an electron with spin σ at site i, $n_{i\sigma} = c_{i\sigma}^+ c_{i\sigma}$ and $n_i = n_{i\uparrow} + n_{i\downarrow}$. $\langle ij \rangle$ denotes nearest neighbours, t is the hopping parameter, U and V are the on-site and inter-site Coulomb repulsion, respectively. We divide the hypercubic lattice into two sublattices such that points on one sublattice have only points of the other sublattice as nearest neighbours. The sublattice is denoted by subscript A or B: $c_{i\sigma} = a_{i\sigma}$ ($b_{i\sigma}$) if $i \in A$ ($i \in B$). Performing a mean-field decoupling of the V-term, we get

$$H = \sum_{i \in A, \sigma} zVn_B a_{i\sigma}^+ a_{i\sigma} + U \sum_{i \in A} n_{i\uparrow} n_{i\downarrow} + \sum_{j \in B, \sigma} zVn_A b_{j\sigma}^+ b_{j\sigma}$$
$$+ U \sum_{j \in B} n_{j\uparrow} n_{j\downarrow} + t \sum_{\langle ij \rangle \sigma}(a_{i\sigma}^+ b_{j\sigma} + b_{j\sigma}^+ a_{i\sigma}) - \tfrac{1}{2} zNVn_A n_B, \tag{2}$$

where z is the number of nearest neighbours, $n_{A/B}$ is the averaged electron occupation number in the A/B sublattice, N is the number of sites in the lattice.

In the alloy-analogue approach the many-body Hamiltonian (2) is replaced by a one-particle Hamiltonian with disorder which is of the form

$$H = \sum_{i \in A, \sigma} E_{A\sigma} a_{i\sigma}^+ a_{i\sigma} + \sum_{j \in B, \sigma} E_{B\sigma} b_{j\sigma}^+ b_{j\sigma} + t \sum_{\langle ij \rangle \sigma}(a_{i\sigma}^+ b_{j\sigma} + b_{j\sigma}^+ a_{i\sigma}) - \tfrac{1}{2} zNVn_A n_B, \tag{3}$$

where

$$E_{A/B,\sigma} = \begin{cases} zVn_{B/A} & \text{with probability } 1 - n_{A/B,-\sigma}, \\ zVn_{B/A} + U & \text{with probability } n_{A/B,-\sigma}. \end{cases} \tag{4}$$

In the following we assume spin-independent expectation values in (4), i.e. we consider only a non-magnetic solution: $n_{\alpha\uparrow} = n_{\alpha\downarrow} = \tfrac{1}{2}n_\alpha$ ($\alpha = A, B$). The Green function G corresponding to the Hamiltonian (3) has to be averaged over all possible configurations of the random potential which can be considered to be due to alloy constituents. The averaging cannot be performed exactly. To solve the alloy problem the CPA is used. The averaged Green

function $\bar{G}$ is obtained from an effective Hamiltonian containing a self-energy $\Sigma_{A/B}(\omega)$ for the A/B sublattice:

$$H_{eff} = \Sigma_A(\omega) \sum_{i \in A, \sigma} a_{i\sigma}^+ a_{i\sigma} + \Sigma_B(\omega) \sum_{j \in B, \sigma} b_{j\sigma}^+ b_{j\sigma} + t \sum_{\langle ij \rangle \sigma} (a_{i\sigma}^+ b_{j\sigma} + b_{j\sigma}^+ a_{i\sigma}). \tag{5}$$

In momentum space the averaged Green functions $\bar{G}_{A/B}(\vec{k}, \omega)$ for the A/B sublattice are of the form

$$\bar{G}_A(\vec{k}, \omega) = \left(\omega - \Sigma_A(\omega) - \frac{t_{\vec{k}}^2}{\omega - \Sigma_B(\omega)} \right)^{-1}, \tag{6}$$

$$\bar{G}_B(\vec{k}, \omega) = \left(\omega - \Sigma_B(\omega) - \frac{t_{\vec{k}}^2}{\omega - \Sigma_A(\omega)} \right)^{-1}, \tag{7}$$

where $t_{\vec{k}}$ is the Fourier transform of the hopping matrix element (the wavevector $\vec{k}$ is for sublattice A (or B)); $\Sigma_{A/B}(\omega)$ are to be determined latter.

The density of states (DOS) for free electrons with the band dispersion $t_{\vec{k}}$ is replaced by the semi-elliptical $\rho_0(\omega) = \frac{2}{\pi W^2} \sqrt{W^2 - \omega^2}$ (we set $W = 1$ as the unit for the energy scale). Note that this model DOS is often used as an additional approximation in combination with the CPA. As was noted in [19], for the Bethe lattice with $3 \leqslant z \leqslant 6$ this approximation is good one, at least in a qualitative sense. The averaged Green functions $\bar{G}_{A/B}(\omega)$ for the A/B sublattice then take the form

$$\bar{G}_A(\omega) = \frac{1}{N} \sum_{\vec{k}} \bar{G}_A(\vec{k}, \omega) = \frac{2}{W^2} \left\{ \omega - \Sigma_B(\omega) - \left[(\omega - \Sigma_B(\omega))^2 - \frac{\omega - \Sigma_B(\omega)}{\omega - \Sigma_A(\omega)} W^2 \right]^{1/2} \right\}. \tag{8}$$

And $\bar{G}_B(\omega)$ is obtained by making the replacement A $\leftrightarrow$ B. A scattering matrix T is introduced for each configuration via

$$G = \bar{G} + \bar{G} T \bar{G}. \tag{9}$$

The CPA demands that the scattering matrix vanishes on average: $\bar{T} = 0$. This yields an expression for $\Sigma_{A/B}(\omega)$ of the form

$$\Sigma_A(\omega) = \bar{E}_A - (zVn_B - \Sigma_A(\omega))\bar{G}_A(\omega)(zVn_B + U - \Sigma_A(\omega)), \tag{10}$$

where $\bar{E}_A = zVn_B + \frac{1}{2}Un_A$. Again $\Sigma_B(\omega)$ and $\bar{E}_B$ are obtained by making the replacement A $\leftrightarrow$ B.

For arbitrary size of the electron density n, we make the following ansatz:

$$n_{A/B} = n \pm x; \qquad \bar{G}_{A/B}(\omega) = G(\pm x, \omega).$$

Eliminating $\Sigma_A(\omega)$, $\Sigma_B(\omega)$ from (8) and (10) leads to an equation for $G(\pm x, \omega)$:

$$\omega - \frac{G(-x, \omega)}{4} - \frac{1}{G(x, \omega)} = zV(n - x) + \frac{U}{2}(n + x)$$

$$- \left[zV(n - x) - \omega + \frac{G(-x, \omega)}{4} + \frac{1}{G(x, \omega)} \right]$$

$$\times \left[zV(n - x) + U - \omega + \frac{G(-x, \omega)}{4} + \frac{1}{G(x, \omega)} \right] G(x, \omega). \tag{11}$$

Setting $x = 0$ in equation (11) and shifting the one-electron energy by $zVn + \frac{U}{2}$, we reproduce the CPA equation for the Green function obtained by Velicky *et al* [20].

If μ is the chemical potential of electrons, then at the temperature T one has

$$n_\alpha = \frac{2T}{N} \sum_{\vec{k},n} \bar{G}_\alpha(\vec{k}, i\omega_n) = -\frac{2}{\pi} \int_{-\infty}^{+\infty} d\omega \, f(\omega) \, \text{Im} \, G(n_\alpha - n, \omega), \qquad (12)$$

where $\omega_n = (2n+1)\pi T$ are the Matsubara frequencies and $f(\omega) = (1 + \exp(\omega - \mu)/T)^{-1}$ is the Fermi function.

The pair of equations (12) must now be solved with the constraint $n_A + n_B = 2n$ for n_A, n_B and μ. For small enough V the solution of (12) is the homogeneous phase with $n_A = n_B$. But if V is sufficiently large it may also be possible to find a CO solution for which $n_A \neq n_B$. One finds that the condition for the onset of CO is equivalent to $n_A = n_B = n$ being a double solution of (12). This condition is expressed as

$$n = -\frac{2}{\pi} \int_{-\infty}^{+\infty} d\omega \, f(\omega) \, \text{Im} \, G(0, \omega), \qquad (13)$$

$$1 = -\frac{2}{\pi} \int_{-\infty}^{+\infty} d\omega \, f(\omega) \, \text{Im} \, G'(0, \omega), \qquad (14)$$

where $G'(0, \omega) = \frac{\partial G(x,\omega)}{\partial x}\big|_{x=0}$ and $G(0, \omega)$ is a solution of (11) when $x = 0$. The latter is a cubic equation for $G(0, \omega)$ and the correct root must be identified from the physical condition for yielding a non-negative DOS. It is also easy to obtain $G'(0, \omega)$ from equation (11). So, for fixed temperature T, on-site Coulomb repulsion U and band filling n, we have the closed system of equations (13), (14) for the critical value V and the chemical potential μ within the framework of the CPA.

3. Numerical results and discussion

We have solved equations (13), (14) numerically; the results may be summarized as follows. In figure 1 we present the phase diagram as a function of n and V for different values of U for the two-dimensional square lattice at zero temperature. The half-bandwidth W was taken as the unit of energy (for the square lattice, $z = 4$ and $W = 4t$). Due to the electron–hole symmetry we consider only $0 \leqslant n \leqslant 1$. From figure 1 one can see that in the two regions ($n \ll 1, n \leqslant 1$) the influences of U on the boundary between the charge-ordered and the homogeneous disordered phase are different: away from half-filling ($n < n^* \approx 0.67$) the on-site interaction U has little effect on the critical value V_c, while for $n^* < n \leqslant 1$ the critical value V_c strongly depends on U. In [15] Dho *et al* found that CO exists over a broad doping range ($0.44 \leqslant x \leqslant 0.8$) in $La_{2-2x}Sr_{1+2x}Mn_2O_7$. It is worth noting that for large U in the same filling region the CPA values of V_c are close to the minimum value (V_c has a minimum at $n^* \approx 0.67$). Although the mechanism of the CO in the layered manganites is more complex than that of the CO induced by a nearest-neighbour Coulomb repulsion, from the above result we may speculate that the CPA is able to describe the CO boundary in this compound. In addition, the advantage of the CPA is that by using this simple approach one can easily obtain phase diagrams in the V–n plane for arbitrary U as well as in the U–V plane at arbitrary n. As an illustration of our approach, in the following we consider the CO transition on the square lattice at quarter-filling ($n = 1/2$). The inset in figure 2 shows the U–V phase diagram at zero temperature. We compare CPA result to the ones obtained by other methods. At $U = \infty$ the critical values $V_c = 0.195W$ and $0.172W$ obtained in [10] by the slave boson approach with a constant DOS and the actual DOS $\rho_0(\omega)$, respectively, are in good agreement with our result $V_c = 0.218W$. At $U = 2W$, $V_c = 0.66W$ was obtained in [9] for the EHM in infinite dimension by the numerical renormalization group (NRG) method, while the CPA result for our 2D lattice is $V_c = 0.237W$.
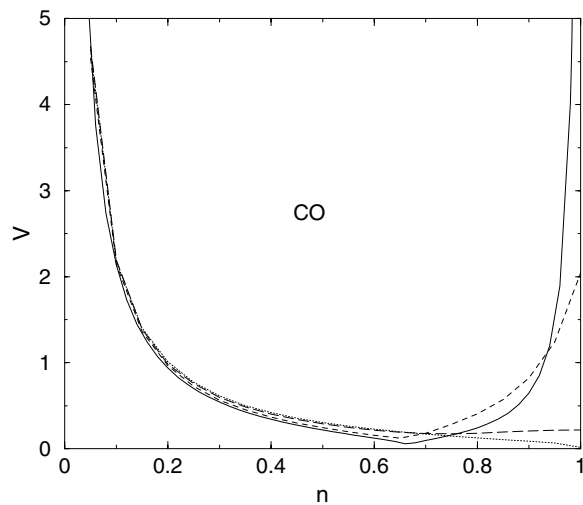
Figure 1. The V–n phase diagram for the 2D EHM ($W = 1$, $T = 0$) for different values of U: $U = 0, 0.5, 1.5$ and ∞ correspond to the dotted, long-dashed, dashed and solid curves, respectively.
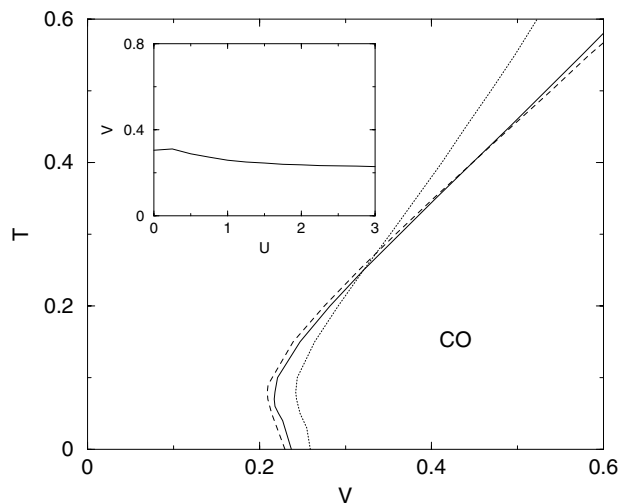

Figure 2. The T–V phase diagram at quarter-filling for several values of U: $U = 1, 2$ and 3 correspond to the dotted, solid and dashed curves, respectively. The inset shows the U–V phase diagram for $n = 1/2$ and $T = 0$.

In [10] McKenzie *et al* argue that in the large-U limit at quarter-filling the charge-ordered phase is destroyed below a critical non-zero value V_c, of the order of t, while we can now show (see the inset of figure 2) that the critical value V_c is almost independent of U; therefore V_c is of the order of t for all values of U. Figure 2 shows the T–V phase diagram for different values of U. For each value of U, re-entrant behaviour as a function of temperature is seen for some region of V. For V in this range, the ground state is homogeneous but a charge-ordered phase exists at intermediate temperature. Note that a re-entrant transition is apparently not obtained by Hartree–Fock approximation in the EHM without electron–phonon interaction.
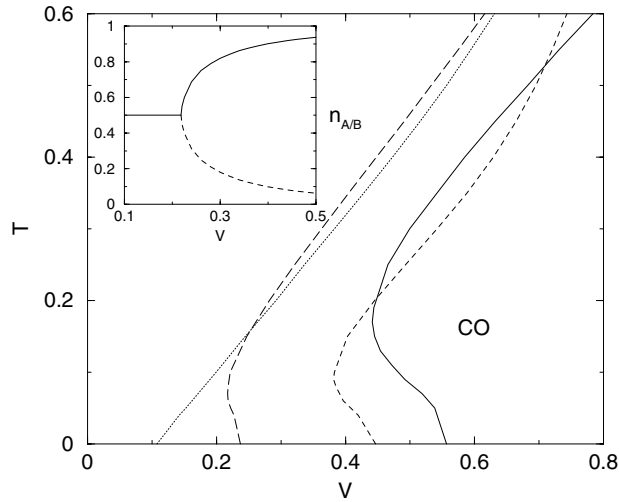
Figure 3. The T–V phase diagram for $U = 2$ at various values of n: $n = 0.3, 0.5, 0.65$ and 0.8 correspond to the solid, long-dashed, dotted and dashed curves, respectively. The inset shows the lattice occupancies n_A (solid curve) and n_B (dashed curve) as a function of V for $U = \infty$ and $T = 0$.

Figure 3 shows the T–V phase diagram for $U = 2$ at different band fillings n. The re-entrant behaviour is seen clearly for the values of n where $V_c(T = 0)$ is larger (e.g. $n = 0.3, 0.8$), while for values of n where $V_c(T = 0)$ is small (e.g. $n = 0.65$), the re-entrant behaviour is not seen.

In the inset in figure 3 we present the CPA result for the V-dependence of the sublattice occupancies n_A and n_B and hence the charge order parameter $(n_A - n_B)$ in the strong-correlation limit $U \to \infty$ at zero temperature. The transition is clearly continuous, in contrast to the result for $U = 2, T = 0$ in [9] where the NRG method gives a first-order phase transition. Note that in the strong-correlation limit $U \to \infty$ from equation (11) one can find an analytic expression for $G(x, \omega)$. Then equations (12) have to be solved self-consistently to find n_A, n_B and μ. For a given set of these parameters the total energy of the system for various states can be calculated. The state with the lowest energy is the true ground state and determines the spectrum. The CPA result for the spectral functions for A and B for $U = \infty, T = 0$ are shown in figure 4. When $V < V_c \approx 0.218$, the spectral functions for A and B are identical and they are independent of V by shifting all the one-electron energy levels and the chemical potential by $2V$. For $V > V_c$ the spectral functions for A and B change and each spectrum splits into upper and lower subbands. On increasing V, the weight of the lower subband in the A spectrum increases, while that in the B spectrum decreases; the subbands in the spectrum become narrower due to the reduced hopping of electrons in the charge-ordered phase. A CO gap opens and it is given by $\Delta = 2\sqrt{16V^2 x^2 + \gamma}$, where $\gamma = \frac{1}{2}[(1 - \frac{n}{2}) - \sqrt{(1 - \frac{n_A}{2})(1 - \frac{n_B}{2})}]$. In the limit of large V, perfect charge order evolves: $n_A \to 1, n_B \to 0$. Therefore in this limit $x \to 1/2$ and the gap between two peaks Δ is given in CPA by $4V$, as compared to $2V$ obtained by the DMFT in [9].
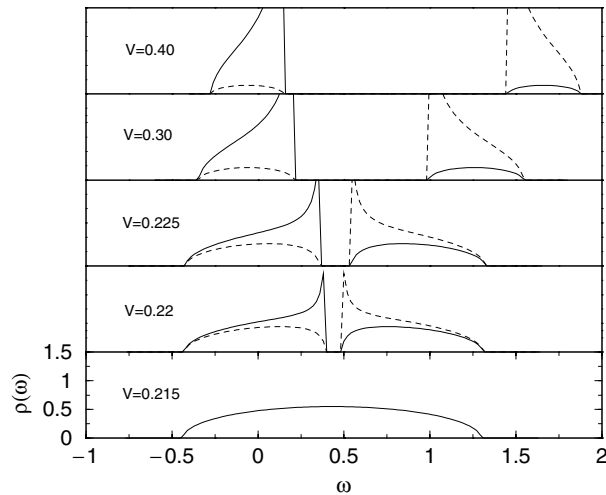
Figure 4. CPA results at quarter-filling for the spectral functions $\rho(\omega)$ for A and B (solid and dashed curves, respectively) for $U = \infty$, $T = 0$ and several values of V. Below the critical value $V_c \approx 0.218$, the spectral functions for the two sublattices are equal.

4. Conclusions

In this paper we have applied the CPA to study CO in the EHM. Within this approximation one can obtain the critical value V_c as a function of temperature T, on-site Coulomb repulsion U and band filling n. To examine the CPA results we consider the CO transition on the 2D square lattice at quarter-filling using a semi-elliptical DOS. It was shown that for all values of U the charge-ordered phase is destroyed below a critical non-zero value V_c of the order of t. Like previous results in [9, 12], our findings indicate a parameter region where the model shows re-entrant behaviour. The re-entrant transition is also observed at other band fillings, as was found experimentally for the layered manganites in [15]. In the strong-correlation limit $U \rightarrow \infty$ at zero temperature, the CPA gives a continuous transition.

Now the CPA is known to give good results for one-particle properties for a wide range of systems. In studying the CO boundary phase in the EHM the CPA has the advantage over DMFT of being analytically simple, and over the Hartree–Fock approximation (small U) and slave boson approach ($U \rightarrow \infty$) of being able to describe the whole range of the on-site interaction U. Of course, as for the alloy CPA, the imaginary part of the self-energy does not vanish at the Fermi level at $T = 0$, so we do not obtain a true Fermi liquid and we only expect our CPA to investigate CO in the EHM well at finite temperature.

The calculation presented here can also be applied to the lattice of higher dimensions, or to the EHM in the presence of a weak magnetic field. To include magnetic phases and cluster effects, one has to go beyond the usual alloy CPA. This is left to future work.

Acknowledgments

References

[1] Wigner E 1938 *Trans. Faraday Soc.* **34** 678
[2] Andrei E Y *et al* 1988 *Phys. Rev. Lett.* **60** 2765
[3] Fulde P 1997 *Ann. Phys., NY* **6** 178
[4] Ochiai A, Suzuki T and Kasuya T 1990 *J. Phys. Soc. Japan* **59** 4129
[5] Ohama T *et al* 1999 *Phys. Rev.* B **59** 3299
[6] Chen C H and Cheong S W 1996 *Phys. Rev. Lett.* **76** 4042
[7] Seo H and Fukuyama H 1998 *J. Phys. Soc. Japan* **67** 2602
[8] van Dongen P G J 1994 *Phys. Rev.* B **50** 14 016
[9] Pietig R, Bulla R and Blawid S 1999 *Phys. Rev. Lett.* **82** 4046
[10] McKenzie R H *et al* 2001 *Phys. Rev.* B **64** 085109
[11] Hirsch J E 1984 *Phys. Rev. Lett.* **53** 2327
[12] Hellberg C S 2001 *J. Appl. Phys.* **89** 6627
[13] Tomioka Y *et al* 1997 *J. Phys. Soc. Japan* **66** 302
[14] Chatterji T *et al* 2000 *Phys. Rev.* B **61** 570
[15] Dho J *et al* 2001 *J. Phys.: Condens. Matter* **13** 3655
[16] Yuan Q and Thalmeier P 1999 *Phys. Rev. Lett.* **83** 3502
[17] Hubbard J 1964 *Proc. R. Soc.* A **281** 401
[18] Czycholl G 1986 *Phys. Rep.* **143** 277
[19] Vlaming R and Vollhardt D 1992 *Phys. Rev.* B **45** 4637
[20] Velicky B, Kirkpatrick S and Ehrenreich H 1968 *Phys. Rev.* **175** 747